

“Unveiling Plant-Based Antimicrobial Peptides by In Silico Tools”

"Amanpreet Thakur^{1,2} and Puja Gupta^{1*}

1. School of Biosciences, RIMT University, Mandi Gobindgarh,
Sirhind, Punjab, India

2. Department of Health sciences, RIMT University, Mandi Gobindgarh,
Sirhind, Punjab, India

*Corresponding author: pujagupta.metagenomics@gmail.com

Abstract

Bacterial vaginosis (BV) arises from a disruption in the vaginal microbiome, primarily characterized by a decrease in *Lactobacilli* and an overgrowth of bacteria like *Gardnerella vaginalis*. These findings highlight the potential of plant-derived AMPs as novel, effective treatments for BV, offering a pathway to combat antimicrobial resistance and recurrence. In silico study was conducted to screen and characterize AMPs from *Thymbra capitata* and *Zataria multiflora*, two plants with well-documented medicinal properties designed to target the ABC transporter permease protein in *G. vaginalis*, a key contributor to antimicrobial resistance. Structural and physicochemical analyses were conducted to assess peptide stability, hydrophilicity, and membrane interaction potential. Analysis revealed that TCCP-1, a peptide from *T. capitata*, is more stable and hydrophilic, while ZMLP-2 from *Z. multiflora* exhibits higher hydrophobicity, making it more suited for membrane interactions. These characteristics suggest that these plant-derived peptides have properties favorable for treating BV. Plant-derived antimicrobial peptides (AMPs), especially those from *T. capitata* and *Z. multiflora*, show potential as innovative treatments for bacterial vaginosis (BV), offering a holistic and effective approach while mitigating antimicrobial resistance and recurrence. In silico analysis suggests that the identified transporter in *G. vaginalis* is likely an integral membrane protein, a critical insight for docking studies as interactions with membrane-bound proteins differ from those in the cytoplasm or extracellular space. Targeting this protein with AMPs could disrupt cellular transport and division, impairing the pathogen's ability to survive and propagate.

Key words: Bacterial vaginosis (BV), antimicrobial Peptides (AMPs), *Gardnerella vaginalis*, *Thymbra capitata*, *Zataria multiflora*, antimicrobial Resistance

Introduction

Bacterial vaginosis (BV) is the most common vaginal infection among women of reproductive age, affecting 40% to 50% of women that can lead to pelvic inflammatory disease. It increases the risk of sexually transmitted infections (STIs) and preterm delivery in pregnant women (Go et al. 2006, Deese et al. 2018, Russo et al. 2019). BV results from an imbalance in the vaginal microbiome, characterized by a reduction in Lactobacilli and an overgrowth of bacteria like *Gardnerella vaginalis*. Although it is not classified as an STI but sexual activity, including multiple partners and practices like douching, can contribute to its development. BV affects

women worldwide, with varying prevalence depending on factors like region, ethnicity, and socioeconomic status (Abou Chacra et al. 2022).

Standard treatments for BV include antibiotics like metronidazole and clindamycin, which have high cure rates but suffer from frequent recurrences due to bacterial biofilms and antibiotic resistance. Herbal remedies like *Allium sativum* show potential in reducing biofilm formation and recurrence (Najafi et al. 2019). Antimicrobial peptides (AMPs) from plants and animals offer a promising alternative by targeting microbial membranes without inducing significant resistance or harming host cells. These peptides also disrupt biofilms and boost immune responses, potentially providing a longer-lasting solution for treating BV and related infections (Javed et al. 2019, Greenbaum et al. 2019).

This study uses in silico tools and algorithms to screen and characterise antimicrobial peptides from specific plant species. *Thymbra capitata* and *Zataria multiflora* are both aromatic plants belonging to the Lamiaceae family that are well-known for their strong antimicrobial qualities, especially against fungal and bacterial infections. According to Shokri and Sharifzadeh (2017), *Z. multiflora* includes thymol, carvacrol, and p-cymene, which have potent antibacterial and antifungal properties against strains of *Candida albicans*, *E. coli* and *S. aureus* inhibiting the production of biofilms. It works especially well against resistant strains (Shokri and Sharifzadeh 2017). There has also been emphasis on its potential for treating vaginal infections due to candida (Rezaie Keikhaie et al. 2018). *T. capitata*, also referred to as conehead thyme, has broad-spectrum antibacterial activity against pathogens such as *C. albicans*, *E. coli* and *S. aureus* due to high carvacrol and thymol. These former mentioned plants are resistant to many drugs due to its effectiveness against many pathogenic strains and its ability to dissolve biofilms (Raut and Karuppaiyil 2016, Almeida et al. 2022). Besides *T. capitata* has also been investigated for its potential to increase shelf life and serve as a natural preservative in food preservation (Soković et al. 2010). Both plants are still gaining popularity because of their ability to treat respiratory and gastrointestinal illnesses as well as their wider uses in food and medical goods. According to research, they have the potential to be used in pharmaceutical formulations that fight microbial illnesses while having fewer side effects than traditional antibiotics (Delgado-Adámez et al. 2017).

In the present study, an attempt has been made to screen and characterize antimicrobial peptides from selected plant species by in silico methods. Besides the interaction of AMPs with microbial membranes has also been predicted. Such studies helps to understand the mechanism of action, optimize stability, solubility, and resistance to proteolytic degradation.

Materials and Methods

Target Selection and localization: The non-redundant proteome of *G. vaginalis* was analyzed using the BLAST tool to assess similarity with *Homo sapiens*. Predictions were based on machine learning algorithms combined with known localization signals, with higher scores indicating greater confidence. PSORTb (<https://www.psorth.org/psorth/>) was used to analyzing the protein's amino acid sequence for features like signal peptides and transmembrane domains (Yu et al. 2010). Parameters, including organism type, were selected to customize predictions.

Conserved Domains and Functional Motifs: The amino acid sequence of the target protein was uploaded to the InterPro online database (<https://www.ebi.ac.uk/interpro/>) which utilized prediction algorithms such as Pfam, SMART, and TIGRFAMs to identify conserved domains and functional motifs. The output provided a detailed summary of protein families, domains, and associated biological functions (Blum et al. 2021).

Homology Modeling: Swiss-Model (<https://swissmodel.expasy.org/>) was employed for three-dimensional structure prediction due to non-availability of experimental structure for the target protein in the Protein Data Bank (PDB). The target protein's amino acid sequence was submitted to Swiss-Model to search for the suitable homologous templates. A homology model was generated based on sequence alignment with the selected template upon finding a suitable match.

Sample Source for AMP: Plant species, *T. capitata* and *Z. multiflora*, were selected for the design of peptides.

Data Mining and Sequence Retrieval: Protein sequences were obtained from the NCBI database. Selected proteins were analyzed for antimicrobial activity using various prediction tools, including APD3 (Wang, Li, and Wang 2016), CAMPR4 (Gawde et al. 2023), AMPGram (Burdukiewicz et al. 2020), iAMPpred (Meher et al. 2017), DRAMP (Shi et al. 2022) and AMPfun (Chung et al. 2020).

Screening and Designing of Antimicrobial Peptides: Six machine-learning tools were utilized to predict antimicrobial potential. Each tool employs different algorithms and methodologies e.g **APD3** that uses sequence comparison to match query peptides with known AMPs, **CAMPR4:** Utilizes an SVM classifier to score antimicrobial potential based on physicochemical properties, **AMPGram:** Combines multiple classifiers to analyze peptide properties and predict antimicrobial activity, **iAMPpred:** Classifies peptides using SVM and Random Forest algorithms based on structural features, **DRAMP:** Employs sequence alignment and SVM methods to predict antimicrobial potential, **AMPfun:** Applies machine learning to predict functional properties of peptides. The predictions were evaluated for consistency and variability across the tools.

Criteria for Peptide Designing: Peptides were selected based on length (10 to 30 amino acids) and cationic surface charge (+3 to +6), primarily derived from natural sources, indicating potential antimicrobial and therapeutic activities.

Structure Prediction and Visualization: The primary structure was analyzed using the PEP Draw tool, while secondary structures were predicted by using PEP 2D tool. The 3D conformations were modelled with PEPFOLD tool (Shen et al. 2014).

Physicochemical Characterization of Peptides: The physicochemical properties, crucial for assessing antimicrobial efficiency and therapeutic potential, were analyzed through a systematic in silico approach. Various properties, such as charge, size, amphipathicity, and solubility, were examined using multiple tools.

Amphipathicity and Other Properties: Tools like PepCalc (Lear and Cobb 2016) and Peptide 2.0 (de la Torre and Albericio 2020) were utilized to evaluate the properties of proposed peptides.

Toxicity Analysis of Peptide Sequence: Peptide sequences were checked for toxicity using the toxin-pred tool, which suggests mutations to adjust toxicity levels (F. Khan, Srivastava, and Kumar 2019). OSIRIS tool was used to supplement the results obtained by toxin-pred tool and both tools shows nontoxic, non-carcinogenic nature of both peptides with no any reproductive irritant behavior (Mukadam and Jagdale 2024).

Analysis of Hemolytic Activity: The HemoPI tool was used for in silico analysis of hemolytic activity, predicting interactions with red blood cell membranes based on the Prob score (Win et al. 2017).

Proteolytic stability and half-life: The proteolytic stability and half-life predicted by peptide cutter and HLP tool (Di 2015).

Identification of signal peptide: SignalP 6.0 was used in this investigation to examine the amino acid sequences of the relevant antimicrobial peptides. The SignalP server received the sequences and evaluated if signal peptides were present, which help these peptides be secreted into particular compartments or outside of cells. Predictions for the signal peptide's cleavage site were given by the tool, along with confidence scores that showed the reliability (Teufel et al. 2022).

Computational Assessment of Drug-Likeness: The ADMET Lab was used in this investigation to evaluate the safety profiles and drug-likeness of the discovered antimicrobial peptides. After the peptide sequences were entered into the ADMET Lab interface, several ADMET metrics, including as solubility, permeability, metabolic stability, and possible toxicity, were computed. Because these predictions were based on well-established datasets and methods, it was possible to thoroughly assess the peptides' eligibility for additional development (Dong et al. 2018).

Peptide Synthesis: Based on the findings, two peptide sequences TCCP 1 and ZMLP 2 were synthesized and evaluated for stability against proteases.

Results

In this study, we performed an in-depth analysis of the proteome of the reference strain of *G. vaginalis* utilizing a genomic approach. The workflow and subsequent analyses, include molecular docking and ADMET analysis, are outlined below.

Drug target selection: A total of 197 proteins from the non-redundant proteome of *G. vaginalis* were search in BLAST tool for similarity with homosapiens. Subsequent analysis focused on this common dataset and 150 proteins were identified as non-homologous to humans. Out of these proteins, efflux ABC transporter, permease protein was subsequently used for selecting the final drug target for virtual screening, marking a crucial step forward in the drug discovery process.

Prediction of location of target protein by tool PSORTb: The tool analysis strongly indicates that the efflux ABC transporter, permease protein is most likely a cytoplasmic membrane protein (Figure 1a).



PSORTb Results (Click here for an explanation of the output formats)

```
SeqID: KXA17501.1 efflux ABC transporter, permease protein [Gardnerella vaginalis]
Analysis Report:
CMSVM+      CytoplasmicMembrane      [No details]
CWSVM+      Unknown                  [No details]
CytoSVM+    Unknown                  [No details]
ECSVM+      Unknown                  [No details]
ModHVM+     CytoplasmicMembrane      [4 internal helices found]
Motif+      Unknown                  [No motifs found]
Profile+    Unknown                  [No matches to profiles found]
SCL-BLAST+ Unknown                  [No matches against database]
SCL-BLASTe+ Unknown                  [No matches against database]
Signal+     Unknown                  [No signal peptide detected]

Localization Scores:
Cytoplasmic      0.00
CytoplasmicMembrane 10.00
Cellwall         0.00
Extracellular    0.00
Final Prediction:
CytoplasmicMembrane 10.00
```

Figure 1a: The PSORTb result in the image provides a localization prediction for the target protein efflux ABC transporter, permease from *G. vaginalis* (SeqID: KXA17501.1).

Functional Domain prediction in target protein Interpro tool: The result obtained strongly support that the efflux ABC transporter permease protein is localized to the cytoplasmic membrane, where it likely functions as part of a transport system, likely involved in the efflux of substances out of the bacterial cell (**Figure 1b**).

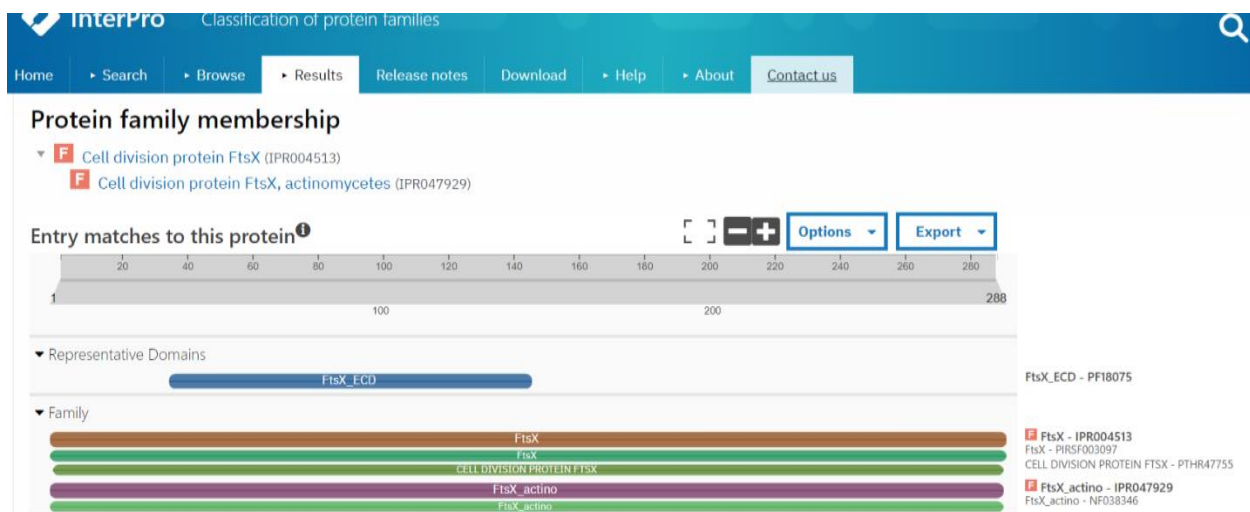


Figure 1b: Localization and Functional Role of ABC Transporter Permease in *G. vaginalis*

Source for Antimicrobial peptide: *T. capitata* and *Z. multiflora* were selected for designing antimicrobial peptides against *G. vaginalis*.

Antimicrobial peptide prediction using machine learning-based prediction tools: The antimicrobial potential of **Peptide 1** and **Peptide 2** was analyzed using six machine learning-based prediction tools: APD3, CAMPR4, AMPGram, iAMPpred, DRAMP, and AMPfun. These results suggest that Peptide 2 may have some antimicrobial activity, but it is much weaker and less consistent than Peptide 1, especially given the very low score from iAMPpred (**Table 1**).

Table 1: Peptide 1 shows much stronger and more consistent antimicrobial activity across all tools, while Peptide 2 demonstrates lower and more variable potential. Peptide 1 appears to be a more reliable candidate for antimicrobial applications, with its high scores across most prediction tools.

TOOL NAME	APD3	CAMPR4	AMPGram	iAMPpred	DRAMP	AMPfun
Peptide 1	AMP	0.86	0.90	0.95	0.67	0.6-0.7
Peptide 2	AMP	0.87	0.52	0.029	0.53	0.6

Structure modeling of target protein: The SWISS-MODEL used efflux ABC transporter, permease protein (GenBank: KXA17501.1) as a template to create a 3D structure of efflux ABC transporter, permease protein (Figure 2). The template belonged to *G. vaginalis* bacterium. The sequence identity between the amino acid sequences of efflux ABC transporter, permease and the reference sequence was 78.05%. Global Model Quality Estimate (GMQE), reflects the overall quality of the model based on various factors and a score close to 1 (in this case 0.89) indicates good model quality. The Ramachandran plot analysis of the protein structure indicates excellent stereochemical quality. A remarkable 96.6% of the non-glycine and non-proline residues are located in the most favored regions, surpassing the standard threshold of 90% for a high-quality model. Additionally, 3.4% of residues are found in the additional allowed regions, which are still geometrically acceptable. Importantly, there are no residues in the generously allowed or disallowed regions, indicating that the model has no problematic conformations. Out of a total of 287 residues, 15 are glycine and 8 are proline, both treated separately due to their unique flexibility and rigidity. Overall, the protein model demonstrates exceptional backbone geometry, making it a reliable structure for further analysis.

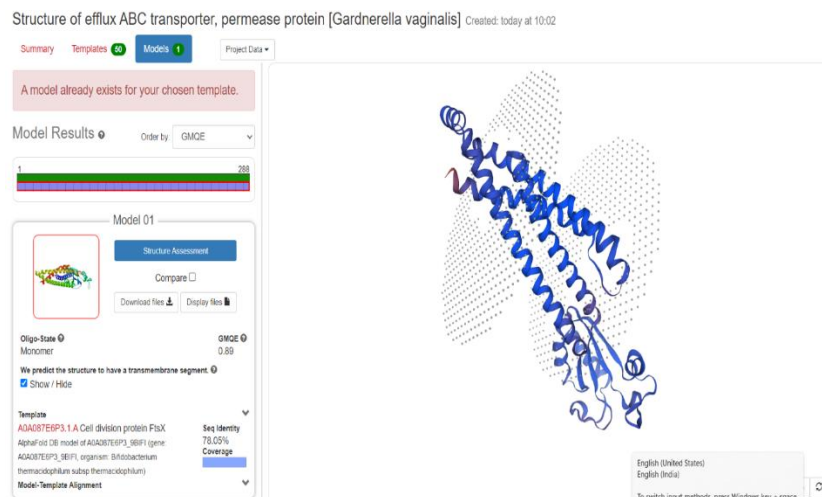


Figure 2: Structure prediction of target protein predicted by Swiss modeling

Primary Structure of peptide: The primary structure of TCCP-1 and ZMLP-2 was drawn by using the PEP draw tool. The sequences are represented as linear chains of amino acids, with each residue labeled according to the standard single-letter amino acid code. TCCP-1 consists of 14 amino acids CRLIRRRGRIRVIC sequence and is characterized by modification in particular amino acids with cyclic structure to increase the stability of peptides. ZMLP-2 is composed of 24 amino acids, displaying a sequence RLSGHILRCMVHACLPLGATRSSW with modification in amino acid sequence to enhance the activity (Table 2)

Table 2: Designed Antimicrobial Peptides Targeting the Efflux ABC Transporter in *G. vaginalis*

S.No.	Peptide name	Peptide Sequence	No. Of Amino Acids
1.	TCCP-1	CRLIRRRGRIRVIC	14
2.	ZMLP-2	RLSGHILRCMVHACLPLGATRSSW	24

Secondary structure prediction by PEP2D tool: The secondary structure of the lead TCCP-1 and ZMLP-2 construct was predicted from the online server PEP2D tool. The PEP2D predictions reveal distinct structural differences between the peptides TCCP-1 and ZMLP-2. TCCP-1 displays a balanced mix of 14.29% helix, 35.71% sheet, and 50.00% coil, suggesting a flexible yet structured conformation that could contribute to stable interactions with other molecules. In contrast, ZMLP-2 shows predominantly coil (83.33%) with minimal sheet (16.67%) and no helical content, indicating a largely unstructured and flexible nature. These differences imply that TCCP-1 may be more stable and suited for specific interactions, while ZMLP-2's flexibility could play a role in dynamic or conformationally adaptive functions.

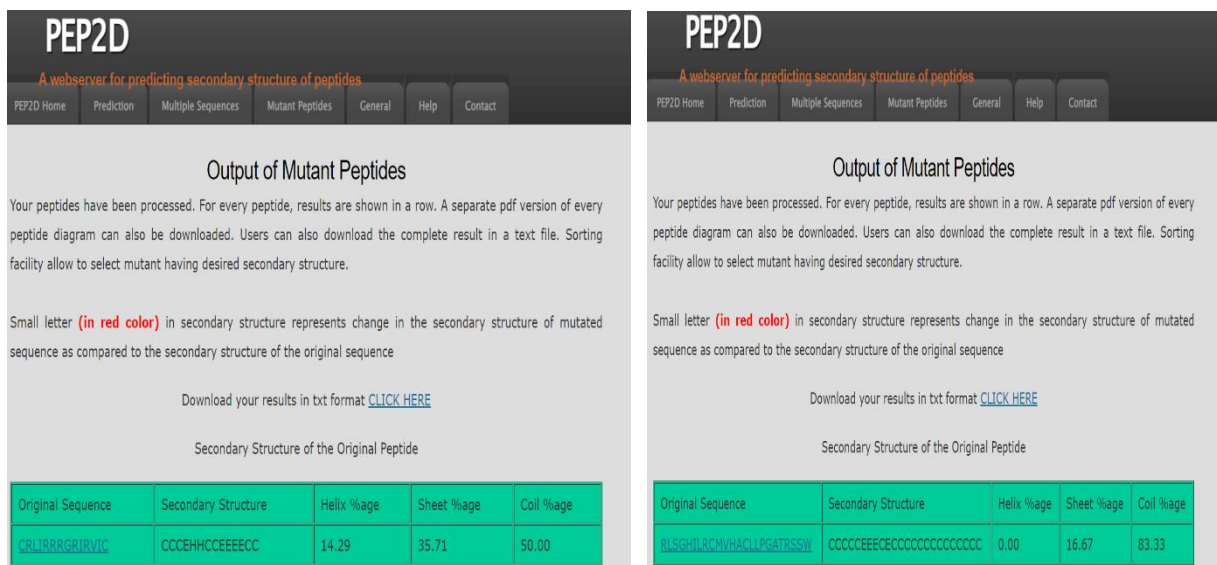


Figure 3: Secondary Structure of Peptide-1 (left) and Peptide-2 (right) predicted by using the PEP2D tool

Tertiary structure prediction: The predicted tertiary structures of Peptide 1 and Peptide 2, modeled using the PEPFOLD 3 tool, reveal distinct folding patterns. Both structures are represented in a cartoon style with a rainbow color gradient from the N-terminus to the C-terminus. Peptide 2 shows a more complex structure, with a well-defined alpha-helix highlighted in green and yellow, while loop regions are represented in red and orange. This suggests a more extensive folding pattern with potential stability. Peptide 1, on the other hand, adopts a simpler fold, with a shorter alpha-helix colored in green to blue, and fewer loop regions in yellow to red, indicating a more compact conformation. No beta-sheets were observed in both peptides structure. These predicted lowest-energy conformations provide insights into the structural stability and potential biological function of each peptide, with the color-coded regions aiding in identifying the distribution of helices and loops.



3 D Confirmation of peptide 1

3 D Confirmation of peptide 2

Figure 4: Tertiary structures of Peptide-1 on (left) and Peptide-2 (right), visualized by using PEPFOLD-3 tool, alpha-helix colored in green to blue and loop regions in yellow to red.

Physicochemical Characterization of Peptide

Hydropathy and Solubility: Peptide 1 (TCCP-1) displayed better water solubility and a strong positive charge (pI = 12.8), making it well-suited for biological interactions in aqueous environments. In contrast, Peptide 2 (ZMLP-2) showed lower solubility and a more hydrophobic character, suggesting it may be more effective in hydrophobic environments such as bacterial membranes (Table 3). Peptide 1 is more hydrophilic, highly basic, and readily soluble in water. Peptide 2 is more hydrophobic, has lower basicity, and requires stronger solvents for solubility, making it better suited for membrane interactions or hydrophobic environments.

Table 3: Hydropathy, Solubility and hydrophobic of designed antimicrobial peptides by Peptide 2.0 Tool

Property	Peptide-1	Peptide-2
Disulfide Connectivity	Cys1 - Cys14	Not indicated
Number of Residues	14	24
Molecular Weight	1768.22 g/mol	2665.18 g/mol
Extinction Coefficient	120 M ⁻¹ cm ⁻¹	5690 M ⁻¹ cm ⁻¹
Isoelectric Point (pI)	12.8	10.36
Net Charge at pH 7	6	3.1
Estimated Solubility	Good water solubility	Poor water solubility
Hydropathy	Mostly hydrophilic	More hydrophobic
Hydrophobicity	35.71%	45.83%
Acidic	0%	0%
Basic	42.86%	20.83%
Neutral	21.43%	33.33%
Solvent recommendation	Water, then acetic acid, TFA	Water, then acetic acid, TFA

Hemolytic Activity: The Prob Score (Probability Score) indicates the likelihood that a peptide will exhibit hemolytic activity, meaning its potential to disrupt or lyse red blood cells (RBCs). This score ranges from 0 to 1, with 0 signifying no hemolytic potential (non-hemolytic) and 1 indicating high hemolytic potential (likely to cause hemolysis). A score closer to 1 implies a higher risk of RBC damage, while a score near 0 suggests a safer peptide with minimal hemolytic activity, which is crucial in determining whether a peptide is suitable for therapeutic use or if modifications are needed. The hemolytic activity prediction is moderate for both peptides with a PROB score of 0.48. However, Peptide 1 (TCCP-1), with its higher amphiphilicity (1.05), charge (6.00), and lower molecular weight (1770.40 Da), is more likely to interact strongly with RBC membranes due to enhanced electrostatic forces and membrane insertion capabilities, potentially leading to higher hemolytic activity. In contrast, Peptide 2 (ZMLP-2), with higher hydropathicity (0.34) and lower charge (3.00), may exhibit weaker membrane disruption and potentially lower hemolytic activity. Despite both peptides sharing the same PROB score, Peptide 1 is predicted to have stronger hemolytic effects due to its more favorable physicochemical properties for membrane interaction (Table 4).

Table 4: Hemolytic activity of peptides predicted using the HemoPI tool

Feature	Peptide-1 (TCCP-1)	Peptide-2 (ZMLP-2)
PROB Score (Original)	0.48	0.48
Hydrophobicity (Original)	-0.5	-0.09
Steric Hindrance (Original)	0.72	0.64
Solvation (Original)	-0.2	0.62
Hydropathicity (Original)	-0.06	0.34
Amphiphilicity (Original)	1.05	0.72
Hydrophilicity (Original)	0.52	-0.4
Net Hydrogen (Original)	24	19
Charge (Original)	6	3
pI (Original)	12.01	10.43
Mol Wt (Original)	1770.4	2685.51

Cytotoxicity prediction

Cytotoxicity prediction by Toxin pred tool: Both peptides were predicted to be non-toxic, with TCCP-1 displaying greater stability in biological environments. TCCP-1's hydrophilic properties, lower molecular weight, and higher positive charge make it more suitable for therapeutic applications. It exhibited a higher hydrophilicity (0.52) and lower hydrophobicity (-0.50) compared to ZMLP-2, as well as a smaller molecular weight (1770.44) and a higher positive charge (6.00). In contrast, ZMLP-2's slight hydrophobicity (-0.09) and higher molecular weight (2665.55) may make it better suited for membrane interactions. It displayed lower hydrophilicity (-0.40) and a higher hydropathicity (0.34), with a positive charge of 4.00. Although both peptides are non-toxic, their different properties suggest distinct potential therapeutic uses.

Cytotoxicity prediction

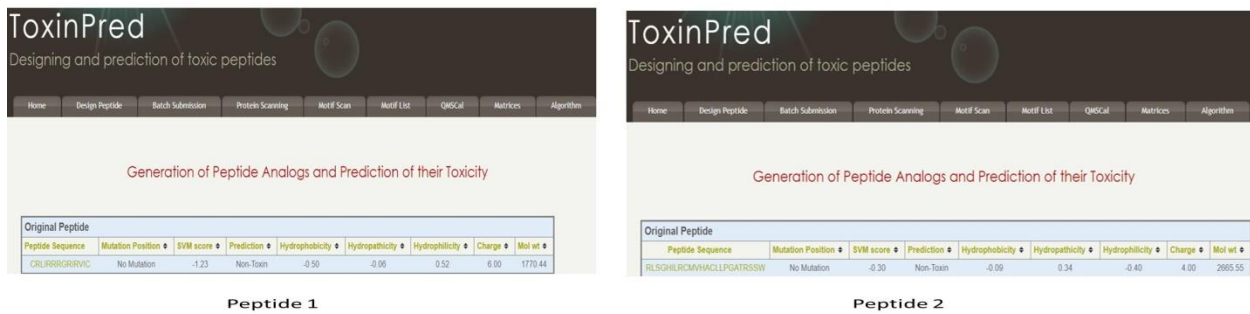


Figure 5a: Cytotoxicity activity of Peptide-1 on (left) and Peptide-2 on (right) predicted by using the Toxin pred tool

Cytotoxicity prediction by OSIRIS tool

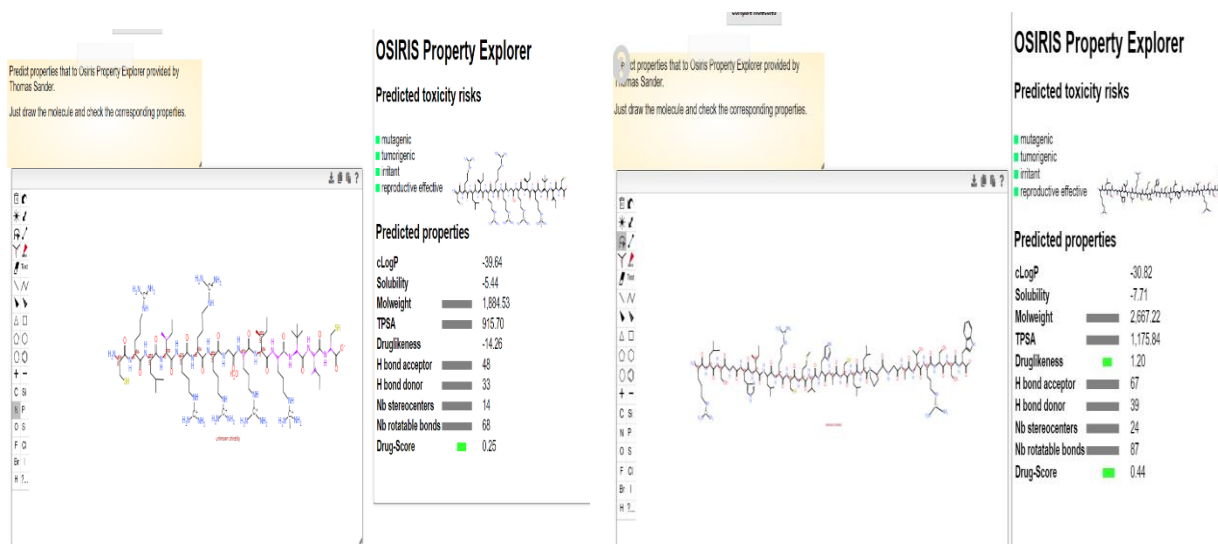


Figure 5b: The analysis of the peptide-1(left) and peptide-2 on (right) sequence using the OSIRIS Property Explorer reveals that both peptides are predicted to have no significant toxicity risks, with no warnings for mutagenic, tumorigenic, irritant, or reproductive effects.

Moreover, the peptide-1 possesses 48 hydrogen bond acceptors and 33 hydrogen bond donors, which highlights its potential for strong interactions with water and biological targets. This high capacity for hydrogen bonding can enhance solubility but may hinder membrane permeability. The structure of the peptide 1 is moderately complex, as indicated by the presence of 14 stereocenters and 68 rotatable bonds, which could affect its interaction with biological targets. The drug score of 0.25, although modest, suggests that the peptide may still have potential for drug development, but significant modifications would likely be required to improve its formulation, delivery, and overall drug-like properties. In summary, while the peptide shows no major toxicity risks, its hydrophilic nature, poor permeability, and low drug likeness score present challenges that would need to be addressed to enhance its viability as a therapeutic candidate.

The molecular weight of 2,667.22 suggests that the peptide-2 is relatively large, which might affect its bioavailability. Despite these issues, the drug likeness score of 1.20 and drug score of 0.44 indicate some potential for the peptide in drug development, provided that delivery and formulation challenges can be addressed. The peptide also shows a high number of hydrogen bond acceptors (67) and donors (39), which may facilitate interactions with biological targets, but its stereochemical complexity (24 stereocenters) and a high number of rotatable bonds suggest significant flexibility, which could influence its conformational stability and interaction specificity. Overall, while the peptide presents some favorable characteristics for drug development, its high hydrophilicity and poor solubility may pose hurdles that require optimization.

Proteolytic stability and half-life of peptide: The two peptide sequences, CRLRRRGGGRIVIC (14mer), and RLSGHILRCMVHACLLPGATRSSW (24mer), show different characteristics in terms of stability and biochemical properties. A normal half-life value is approximately 0.500–1.000 seconds for peptides in intestine-like environments. The 24-mer peptide has a half-life of 0.534 seconds, which falls within the normal range, while the 14-mer peptide has a slightly longer half-life of 0.892 seconds, indicating higher stability in this environment. Both peptides are classified as having normal overall stability, but the 14mer shows greater relative stability (3.321) compared to the 24mer (3.008). Additionally, the 14mer is more hydrophobic (16.171 KJ/mol) than the 24mer (1.525 KJ/mol), suggesting stronger non-polar interactions. The 14mer also has a higher charge (6.000 vs. 0.400 for the 24mer), which may affect its solubility and behavior in biological environments. The 24mer is larger, with a higher molecular weight (2665.550 g/mol vs. 1770.440 g/mol for the 14mer), and has a slightly lower isoelectric point (6.585 vs. 7.900), meaning it behaves differently at various pH levels. Both peptides have normal thermodynamic properties, but the 14mer may be more favorable for dissolution in water due to its lower free energy of solution.

Proteolytic stability			
Name of enzyme	No. of cleavages	Positions of cleavage sites	
Arg-C protease	6	2 5 6 7 9 11	
Chymotrypsin-low specificity (C-term to [FYWM], not before F)	1	3	
Neutrophil elastase	1	12	
Pepsin (pH=3)	1	3	
Pepsin (pH=2)	1	3	
Protease K	5	3 4 10 12 13	
Thermolysin	5	2 3 9 11 12	
Trypsin	5	2 5 7 9 11	

Proteolytic stability			
Name of enzyme	No. of cleavages	Positions of cleavage sites	
Arg-C protease	3	1 6 21	
Chymotrypsin-high specificity (C-term to [FYW], not before F)	1	24	
Chymotrypsin-low specificity (C-term to [FYWM], not before F)	7	2 5 7 10 12 15 24	
Neutrophil elastase	3	11 13 16	
Pepsin (pH=3)	2	5 16	
Pepsin (pH=2)	4	2 6 16 24	
Protease K	10	2 6 7 11 13 15 16 19 20 24	
Thermolysin	6	1 5 6 9 10 12 14 16	
Trypsin	3	1 6 21	

The selected enzymes do not cut:

- Caspase1
- Caspase10
- Caspase3
- Caspase4
- Caspase6
- Caspase7
- Chymotrypsin-high specificity (C-term to [FYW], not before F)
- Enteropeptidase
- Glutamyl endopeptidase
- Proline-endopeptidase
- Staphylococcal peptidase 1
- Thrombin

Peptide -1

The selected enzymes do not cut:

- Caspase1
- Caspase10
- Caspase3
- Caspase4
- Caspase6
- Caspase7
- Enteropeptidase
- Glutamyl endopeptidase
- Proline-endopeptidase
- Staphylococcal peptidase 1
- Thrombin

Peptide -2

Figure 6a: Proteolytic stability of Peptide-1 on (left) and Peptide-2 on (right) by Peptide cutter tool

HLP: A webserver for predicting half-life of peptides in intestine like environment

Home | Submit | Peptide, Protein, Batch | Data sets | Algorithm | Help | Links | Team | Contact us

Go Back

Results Peptide Half-life (14mer)

SN	Peptide	Molecular Weight (kDa)	pI	Hydrophobicity (kcal/mol)	Hydrophilicity (kcal/mol)	pKa	pI	Relative stability	Free Energy of Solution (kJ/mol)	Optical Rotation	Energy of Formation	Free Capacity	Relative stability
1	CRLRRRGGGRIVIC	1.770	7.900	16.171	-1.525	6.000	0.400	3.321	1770.440	0.892	0.892	0.892	0.892

HLP: A webserver for predicting half-life of peptides in intestine like environment

Home | Submit | Peptide, Protein, Batch | Data sets | Algorithm | Help | Links | Team | Contact us

Go Back

Results Peptide Half-life (24mer)

SN	Peptide	Molecular Weight (kDa)	pI	Hydrophobicity (kcal/mol)	Hydrophilicity (kcal/mol)	pKa	pI	Relative stability	Free Energy of Solution (kJ/mol)	Optical Rotation	Energy of Formation	Free Capacity	Relative stability
1	RLSGHILRCMVHACLLPGATRSSW	2.666	6.585	1.525	-16.171	0.400	6.000	3.008	2665.550	0.534	0.534	0.534	0.534

Figure 6b: Half-life of Peptide-1 on (left) and Peptide-2 on (right) predicted by HLP tool

4.5. Prediction of signal peptide

SignalP-6.0 - Results

Summary of 1 predicted sequences from eukarya

Predictions list. Use the instruction page for more detailed description of the output page.

Download:

[JSON Summary](#)

[Prediction summary](#)

[Processed entries fasta](#)

[Processed entries gff3](#)

[Region predictions gff3](#)

[All results compressed \(zip\)](#)

Predicted proteins

Protein type	Other	Signal Peptide (Sec/SPI)
_WBU11945.1 ribosomal protein L36_chloroplast_Thymira capitata Prediction: Other	0.9763	0.0237

Instructions - SignalP 6.0

SignalP-6.0 - Results

Summary of 1 predicted sequences from eukarya

Predictions list. Use the instruction page for more detailed description of the output page.

Download:

[JSON Summary](#)

[Prediction summary](#)

[Processed entries fasta](#)

[Processed entries gff3](#)

[Region predictions gff3](#)

[All results compressed \(zip\)](#)

Predicted proteins

Protein type	Other	Signal Peptide (Sec/SPI)
_ATU82842.1 ribosomal protein S14_chloroplast_Zataria multiflora Prediction: Other	0.9999	0.0001

Instructions - SignalP 6.0

Figure 7: The results strongly indicate that this Peptide-1 on (left) and Peptide-2 on (right) do not have characteristics of a typical signal peptide for secretion. It is likely not targeted for transport via the classical secretory pathways (like the Sec pathway), implying that the sequence may be a cytosolic or internal peptide

ADMET Analysis

ADMET lab

Home > Webserver > Prediction Results

Details of the model

- Endpoint: drug likeness
- Method: RandomForest
- Accuracy: 0.801
- AUC: 0.870
- CV fold: 5
- Descriptors: MACCS

Explain: The **Probability** for the **Category** means probability of predicted category 1. The details about how to explain the **Results**, please see here >>

Results

Search:

Category	Probability	Structure
1	0.946	

ADMET lab

Home > Webserver > Prediction Results

Details of the model

- Endpoint: drug likeness
- Method: RandomForest
- Accuracy: 0.801
- AUC: 0.870
- CV fold: 5
- Descriptors: MACCS

Explain: The **Probability** for the **Category** means probability of predicted category 1. The details about how to explain the **Results**, please see here >>

Results

Category	Probability	Structure
1	0.946	

Figure 8: The ADMET lab results indicate that the peptide -1 on (left) predicted to be drug-like with a probability of 94.6% and peptide-2 (right) falls into category 1, indicating drug-likeness, with a high probability of 94.6%.

The ADMETlab results indicate that the peptide 1 has been evaluated for drug likeness using a Random Forest model. The model shows an accuracy of 80.1% and an AUC (Area Under the Curve) of 0.870, signifying good model performance in distinguishing between drug-like and non-drug-like compounds. The descriptors used for this prediction are MACCS fingerprints, which are commonly applied for representing molecular structures. According to the results, the compound is predicted to be drug-like with a probability of 94.6%, indicating a strong likelihood of being classified as a potential drug candidate. On the other hand, for the peptide 2 sequence indicate a high likelihood of being drug-like, based on the Random Forest model. The model maintains an accuracy of 80.1% and an AUC of 0.870, demonstrating reliable performance in distinguishing drug-like compounds. According to the results, the peptide falls into category 1, indicating drug-likeness, with a high probability of 94.6%. This suggests a strong confidence in the classification of the peptide as drug-like. A partial representation of the peptide's molecular structure is also displayed, further supporting the analysis. Overall, the prediction indicates that these peptides have significant potential as a drug-like compound based on the model's evaluate on.

Docking: The results from the HADDOCK docking of your target protein with peptide 1 suggest a reliable interaction, particularly in Cluster 2, which has a HADDOCK score of -50.0 ± 0.7 , indicating strong overall binding. The cluster size of 21 suggests that this conformation occurs frequently among the generated models, making it more likely to represent a valid interaction. The RMSD from the lowest-energy structure is 3.8 ± 0.1 Å, showing that the structures within the cluster are similar but exhibit some variability in positioning. Both Van der Waals energy and electrostatic energy contribute significantly to the stability of the interaction, with values of -33.9 ± 4.3 kcal/mol and -123.4 ± 28.6 kcal/mol, respectively, highlighting favorable close contacts and strong electrostatic forces between the protein and peptide. The desolvation energy is relatively low at 3.2 ± 1.9 kcal/mol, indicating that displacing water molecules does not pose a significant barrier to binding. However, the restraint violation energy of 54.6 ± 21.5 kcal/mol suggests some deviations from the expected conformation, though the standard deviation implies variation across the models in this cluster. The buried surface area of 1008.8 ± 21.0 Å² further supports strong binding, as a substantial portion of the peptide is involved in the interaction. Finally, the Z-score of -1.8 indicates that Cluster 2 is a reliable solution, being 1.8 standard deviations better than the average cluster score. In summary, Cluster 2 represents a promising and stable docking model with strong binding energies, although some restraint violations and structural variability should be noted.

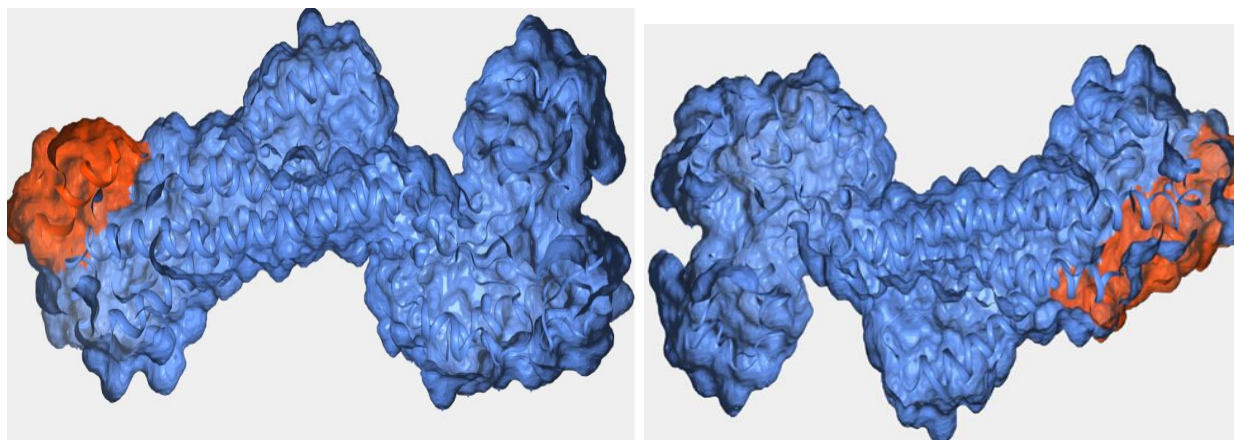


Figure 9: This molecular docking model illustrates the interaction between peptide 1 (on Left) and peptide 2 (on right) depicted in orange and the target protein (shown in blue). The structural alignment of both the peptide and the protein reveals complementary interactions, which likely enhance the stability and affinity of the complex.

The docking results of peptide 2 with the target protein, as analyzed by HADDOCK, indicate a favorable and reliable interaction. Cluster 4, with a HADDOCK score of -60.7 ± 6.7 , represents one of the best docking solutions, suggesting strong binding affinity between the peptide and the protein. The relatively low root-mean-square deviation (RMSD) of $1.0 \pm 0.6 \text{ \AA}$ further supports the consistency of this cluster, indicating that the conformations within the cluster are very similar to the overall lowest-energy structure. Energetically, the interaction is characterized by strong non-covalent forces, reflected in the significant Van der Waals energy of $-42.9 \pm 6.0 \text{ kcal/mol}$ and electrostatic energy of $-42.1 \pm 31.8 \text{ kcal/mol}$. Despite the variability in electrostatic interactions, the desolvation energy of $-28.7 \pm 6.1 \text{ kcal/mol}$ suggests a favorable interaction in the absence of water molecules at the binding interface.

Moreover, the buried surface area (BSA) of $1339.4 \pm 125.6 \text{ \AA}^2$ indicates that a large portion of the peptide is engaged with the protein, which is indicative of a stable and strong interaction. However, the restraints violation energy of $193.6 \pm 46.0 \text{ kcal/mol}$ suggests that some experimental restraints may not be fully respected in certain docking poses, indicating room for improvement in refining the interaction. Overall, with a Z-score of -2.1 , this cluster stands out as one of the more reliable docking solutions, as it deviates significantly from the average cluster, confirming that peptide 2 likely exhibits strong and stable binding to the target protein.

Discussion

In this study, *Thymbra capitata* and *Zataria multiflora* were chosen for peptide sequencing due to their documented antimicrobial and medicinal properties, making them valuable candidates within the Lamiaceae family. This plant family is renowned for its bioactive secondary metabolites, traditionally researched for their essential oils known to exhibit antibacterial, antifungal, and antioxidant activities (S. Khan et al. 2023). However, this research took a novel approach, focusing on the lesser-explored antimicrobial peptides (AMPs) within these plants. With plant-derived AMPs gaining attention as alternatives to conventional antibiotics, these species represent untapped resources for potential therapeutic compounds (Frezza et al. 2019, Dawood et al. 2022). Recent studies have supported this exploration, with findings from other

Lamiaceae plants revealing AMPs with similar antimicrobial efficacy (Tanhaeian, Sekhavati, and Moghaddam 2020).

The investigation led to the identification of two specific peptides: TCCP-1 from *Thymbra capitata* and ZMLP-2 from *Zataria multiflora*. TCCP-1 (CRLIRRRGRIRVIC) stood out due to its high arginine (R) and cysteine (C) content. Arginine-rich peptides interact strongly with bacterial membranes due to their positive charge, which binds effectively to negatively charged bacterial surfaces. Meanwhile, cysteine plays a key role in forming disulfide bonds, stabilizing the peptide's 3D structure, thus enhancing resistance to enzymatic degradation and increasing antimicrobial efficacy (Sohrabi et al. 2024). This structural stability suggests that TCCP-1 could retain its therapeutic potential even under challenging biological conditions.

ZMLP-2 (RLSGHILRCMVHACLLPGATRSSW) from *Zataria multiflora* features a combination of hydrophobic and hydrophilic residues, highlighting its potential for multifunctional activity. Hydrophobic residues, in particular, support interactions with lipid membranes, suggesting that ZMLP-2 could efficiently disrupt bacterial membranes. Like TCCP-1, ZMLP-2's cysteine residues could form stabilizing disulfide bonds, aiding in proteolytic resistance. Its complex sequence hints at potential roles beyond antimicrobial activity, such as antioxidant or enzyme-inhibitory functions (Ashraf et al. 2023). As pathogens develop resistance to traditional antibiotics, AMPs offer promising alternatives due to their unique mechanisms, often disrupting bacterial membranes in ways that are harder for bacteria to resist.

Further analysis explored the efflux systems and membrane transport proteins that may contribute to antibiotic resistance, specifically within *Gardnerella vaginalis*, an opportunistic pathogen. Efflux proteins, like the ABC transporter permease, help expel toxic substances from bacterial cells, enhancing survival in hostile environments, including those with immune responses or antibiotic presence. Targeting this transporter with AMPs may hinder the bacterial cell's ability to resist antibiotics, thus representing a new therapeutic strategy. In silico analysis indicated that this transporter is likely integral to the cell membrane of *G. vaginalis*, a crucial insight for docking studies since interactions with membrane-bound proteins can differ from those within the cytoplasm or extracellular space. The protein's transmembrane helices and lack of signal peptides align with its role in membrane transport, specifically for substrates essential to bacterial function and survival.

Finally, this protein, a member of the ABC transporter family, includes domains that may also regulate cell division, with the FtsX domain suggesting it could be critical for maintaining cell integrity and division in *G. vaginalis*. By targeting this protein, AMPs could potentially disrupt cellular transport and division, impacting the pathogen's ability to thrive.

Conclusion

This study successfully identified and characterized two antimicrobial peptides (AMPs), TCCP-1 from *Thymbra capitata* and ZMLP-2 from *Zataria multiflora*, designed to target the ABC transporter permease protein in *G. vaginalis*, a key contributor to antimicrobial resistance. These peptides were evaluated for their structural, physicochemical, and biological properties. TCCP-1 showed superior antimicrobial potential, with enhanced stability and solubility. Structural

analysis indicated TCCP-1 is more stable and hydrophilic, while ZMLP-2 is more flexible and hydrophobic, favoring membrane interactions.

Acknowledgment

PG and AT are thankful to RIMT, University for support.

Conflicts of interests

There are no conflicts of interest in this work.

References

- Ashraf, Mohammad Vikas, Shreekar Pant, M. A. Hannan Khan, Ali Asghar Shah, Sazada Siddiqui, Mouna Jeridi, Heba Waheeb Saeed Alhamdi, and Shoeb Ahmad. 2023. "Phytochemicals as Antimicrobials: Prospecting Himalayan Medicinal Plants as Source of Alternate Medicine to Combat Antimicrobial Resistance." *Pharmaceuticals* 16 (6): 881. doi:10.3390/ph16060881.
- Blum, Matthias, Hsin-Yu Chang, Sara Chuguransky, Tiago Grego, Swaathi Kandasamy, Alex Mitchell, Gift Nuka, et al. 2021. "The InterPro Protein Families and Domains Database: 20 Years On." *Nucleic Acids Research* 49 (D1): D344–D354. doi:10.1093/nar/gkaa977.
- Burdukiewicz, Michał, Katarzyna Sidorczuk, Dominik Rafacz, Filip Pietluch, Jarosław Chilimoniuk, Stefan Rödiger, and Przemysław Gagat. 2020. "Proteomic Screening for Prediction and Design of Antimicrobial Peptides with AmpGram." *International Journal of Molecular Sciences* 21 (12): 4310. doi:10.3390/ijms21124310.
- Chung, Chia-Ru, Ting-Rung Kuo, Li-Ching Wu, Tzong-Yi Lee, and Jorng-Tzong Horng. 2020. "Characterization and Identification of Antimicrobial Peptides with Different Functional Activities." *Briefings in Bioinformatics* 21 (3): 1098–1114. doi:10.1093/bib/bbz043.
- Dawood, Mahmoud A. O., Mohammed F. El Basuini, Sevdan Yilmaz, Hany M. R. Abdel-Latif, Mahmoud Alagawany, Zulhisyam Abdul Kari, Mohammad Khairul Azhar Abdul Razab, Noor Khalidah Abdul Hamid, Tossapol Moonmanee, and Hien Van Doan. 2022. "Exploring the Roles of Dietary Herbal Essential Oils in Aquaculture: A Review." *Animals* 12 (7): 823. doi:10.3390/ani12070823.
- de la Torre, Beatriz G., and Fernando Albericio. 2020. "Peptide Therapeutics 2.0." *Molecules* 25 (10): 2293. doi:10.3390/molecules25102293.
- Di, Li. 2015. "Strategic Approaches to Optimizing Peptide ADME Properties." *The AAPS Journal* 17 (1): 134–143. doi:10.1208/s12248-014-9687-3.
- Dong, Jie, Ning-Ning Wang, Zhi-Jiang Yao, Lin Zhang, Yan Cheng, Defang Ouyang, Ai-Ping Lu, and Dong-Sheng Cao. 2018. "ADMETlab: A Platform for Systematic ADMET Evaluation Based on a Comprehensively Collected ADMET Database." *Journal of Cheminformatics* 10 (1): 29. doi:10.1186/s13321-018-0283-x.
- Frezza, Claudio, Alessandro Venditti, Chiara Toniolo, Daniela De Vita, Ilaria Serafini, Alessandro Ciccòla, Marco Franceschin, et al. 2019. "Pedicularis L. Genus: Systematics, Botany, Phytochemistry, Chemotaxonomy, Ethnopharmacology, and Other." *Plants* 8 (9): 306. doi:10.3390/plants8090306.

- Gawde, Ulka, Shuvechha Chakraborty, Faiza Hanif Waghu, Ram Shankar Barai, Ashlesha Khandekar, Rishikesh Indraguru, Tanmay Shirsat, and Susan Idicula-Thomas. 2023. "CAMPR4: A Database of Natural and Synthetic Antimicrobial Peptides." *Nucleic Acids Research* 51 (D1): D377–D383. doi:10.1093/nar/gkac933.
- Khan, Fariya, Vivek Srivastava, and Ajay Kumar. 2019. "Computational Identification and Characterization of Potential T-Cell Epitope for the Utility of Vaccine Design Against Enterotoxigenic Escherichia Coli." *International Journal of Peptide Research and Therapeutics* 25 (1): 289–302. doi:10.1007/s10989-018-9671-3.
- Khan, Sohail, Abdullah Abdo, Ying Shu, Zhisheng Zhang, and Tieqiang Liang. 2023. "The Extraction and Impact of Essential Oils on Bioactive Films and Food Preservation, with Emphasis on Antioxidant and Antibacterial Activities—A Review." *Foods* 12 (22): 4169. doi:10.3390/foods12224169.
- Lear, Sam, and Steven L. Cobb. 2016. "Pep-Calc.Com: A Set of Web Utilities for the Calculation of Peptide and Peptoid Properties and Automatic Mass Spectral Peak Assignment." *Journal of Computer-Aided Molecular Design* 30 (3): 271–277. doi:10.1007/s10822-016-9902-7.
- M. Mukadam, Marwa, and Deepali M. Jagdale. 2024. "In Silico ADME/T Prediction of Steroidal Chalcone Derivatives Using Swiss ADME and OSIRIS Explorer." *Research Journal of Pharmacy and Technology* 17 (2): 843–848. doi:10.52711/0974-360X.2024.00130.
- Meher, Prabina Kumar, Tanmaya Kumar Sahu, Varsha Saini, and Atmakuri Ramakrishna Rao. 2017. "Predicting Antimicrobial Peptides with Improved Accuracy by Incorporating the Compositional, Physico-Chemical and Structural Features into Chou's General PseAAC." *Scientific Reports* 7. doi:10.1038/srep42362.
- Shen, Yimin, Julien Maupetit, Philippe Derreumaux, and Pierre Tufféry. 2014. "Improved PEP-FOLD Approach for Peptide and Miniprotein Structure Prediction." *Journal of Chemical Theory and Computation* 10 (10): 4745–4758. doi:10.1021/ct500592m.
- Shi, Guobang, Xinyue Kang, Fanyi Dong, Yanchao Liu, Ning Zhu, Yuxuan Hu, Hanmei Xu, Xingzhen Lao, and Heng Zheng. 2022. "DRAMP 3.0: An Enhanced Comprehensive Data Repository of Antimicrobial Peptides." *Nucleic Acids Research* 50 (D1): D488–D496. doi:10.1093/nar/gkab651.
- Sohrabi, Seyyed Mohsen, Maasume Shahmohammadi, Mohsen Mohammadi, Zahra Abdi, Mohammad Hossein Shams, Sayyad Khanizadeh, and Farnaz Kheirandish. 2024. "Identification and Functional Characterization a Cysteine-Rich Peptide from the Garlic (*Allium Sativum* L.)." *South African Journal of Botany* 166 (March): 690–697. doi:10.1016/j.sajb.2024.02.009.
- Tanhaeian, Abbas, Mohammad Hadi Sekhavati, and Mohammad Moghaddam. 2020. "Antimicrobial Activity of Some Plant Essential Oils and an Antimicrobial-Peptide against Some Clinically Isolated Pathogens." *Chemical and Biological Technologies in Agriculture* 7 (1): 13. doi:10.1186/s40538-020-00181-9.
- Teufel, Felix, José Juan Almagro Armenteros, Alexander Rosenberg Johansen, Magnús Halldór Gíslason, Silas Irby Pihl, Konstantinos D. Tsirigos, Ole Winther, Søren Brunak, Gunnar von Heijne, and Henrik Nielsen. 2022. "SignalP 6.0 Predicts All Five Types of Signal Peptides Using Protein Language Models." *Nature Biotechnology* 40 (7): 1023–1025. doi:10.1038/s41587-021-01156-3.

- Wang, Guangshun, Xia Li, and Zhe Wang. 2016. "APD3: The Antimicrobial Peptide Database as a Tool for Research and Education." *Nucleic Acids Research* 44 (D1): D1087–D1093. doi:10.1093/nar/gkv1278.
- Win, Thet Su, Aijaz Ahmad Malik, Virapong Prachayasittikul, Jarl E. S Wikberg, Chanin Nantasenamat, and Watshara Shoombuatong. 2017. "Hemopred: A Web Server for Predicting the Hemolytic Activity of Peptides." *Future Medicinal Chemistry* 9 (3): 275–291. doi:10.4155/fmc-2016-0188.
- Yu, Nancy Y., James R. Wagner, Matthew R. Laird, Gabor Melli, Sébastien Rey, Raymond Lo, Phuong Dao, et al. 2010. "PSORTb 3.0: Improved Protein Subcellular Localization Prediction with Refined Localization Subcategories and Predictive Capabilities for All Prokaryotes." *Bioinformatics* 26 (13): 1608–1615. doi:10.1093/bioinformatics/btq249.